DOI: 10.3842/umzh.v76i8.7596

UDC 531

Tevfik Şahin[1] (Department of Mathematics, Amasya University, Turkey),
Keziban Orbay (Mathematics and Science Education Department, Amasya University, Turkey),
Zehra Özdemir (Department of Mathematics, Amasya University, Turkey)

A GENERALIZATION FOR THE KINEMATICS OF SLIDING-ROLLING MOTION IN THE SEMI-EUCLIDEAN SPACE $\mathbb{R}^3_\varepsilon$

УЗАГАЛЬНЕННЯ КІНЕМАТИКИ РУХУ КОВЗАННЯ-КОЧЕННЯ В НАПІВЕВКЛІДОВОМУ ПРОСТОРІ $\mathbb{R}^3_\varepsilon$

We propose a generalization for the sliding-rolling motion, which leads to meaningful physical and mathematical results as the general metric includes the time dimension. We also investigate the kinematics of the relative motion of two rigid objects, which maintain sliding-rolling contact, by using the general adjoint approach in the semi-Euclidean space $\mathbb{R}^3_\varepsilon$, where $\varepsilon \in \{0,1\}$. This generalization gives the geometric kinematic equations of the sliding-rolling motion in Minkowski and Euclidean spaces. In these spaces, we get a set of overconstrained equations. Solving this system, we determine translational and angular velocities of the moving surface. Finally, we illustrate the results by two examples.

Наведено узагальнення для руху ковзання-кочення, яке дає вагомі фізичні і математичні результати, оскільки загальна метрика включає часовий вимір. Також досліджено кінематику відносного руху двох твердих об'єктів, що підтримують контакт ковзання-кочення, за допомогою загального спряженого підходу у напівевклідовому просторі $\mathbb{R}^3_\varepsilon$, де $\varepsilon \in \{0,1\}$. Запропоноване узагальнення дає геометричні кінематичні рівняння руху ковзання-кочення у просторах Мінковського та Евкліда. У цих просторах отримано систему рівнянь із надмірними обмеженнями. Розв'язуючи цю систему, ми визначаємо поступальну та кутову швидкості рухомої поверхні. Насамкінець отримані результати проілюстровано двома прикладами.

1. Introduction. Rolling contact between two surfaces plays an important role in robotics and engineering in order to drive a moving surface on a fixed surface such as spherical robots, single wheel robots, and multi-fingered robotic hands. This paper presents a method for sliding-rolling model in Lorentzian geometry. In particular, we are interested in the question how the Lorentzian metric affects the mechanics as the general metric includes the time dimension.

There are important and strong connections between Lorentzian geometry and physics. The Lorentz transformation may include a rotation of space; a rotation-free Lorentz transformation is called a Lorentz boost. In Minkowski space, the Lorentz transformations preserve the spacetime interval between any two events. This property is the defining property of a Lorentz transformation. They describe only the transformations in which the spacetime event at the origin is left fixed. They can be considered as a hyperbolic rotation of Minkowski space. A Lorentz transform is a transformation between two inertial (not accelerating) frames according to special relativity. The time interval between two events can change in a Lorentz transformation. Thus, as both space and time intervals have different values in different frames of reference, the velocity of an object in each of these frames must be observed to be different. This article presents the kinematic formulation using a general framework when two objects maintain the sliding-roll theme. Through this general framework, the effect of the Lorentzian metric on this motion will be given. In Lorentzian space, vectors and thus curves have three different causal characteristics due to their metric structure. Thus, along a curve adjacent to a general surface, the velocity, arc length, and curvatures of the curve

[1] Corresponding author, e-mails: tevfik.sahin@amasya.edu.tr, tevfiksah@gmail.com.

will change due to the time dimension effect. Hence, the kinematics of the two objects maintaining slip-rotation contact will also change. When two moving frames are connected to the contact loci, the metric has an effect on the geometric velocity of a random point on the moving object. By considering the general metric, the velocity of this arbitrary point is found by using the geometric velocity, and the translational and rotational velocity of the object. Then the effect of the Lorentzian metric on the shear-rotational motion was determined by using an extremely constrained system consisting of eight equations with five variables. Later, the angular and translational velocities were obtained by solving this system of equations. Also, a visual example is given to illustrate the Lorentzian approach.

The sliding-spinning-rolling kinematics was derived in [1] by using the Taylor series. Kinematic equations for this motion depending on the velocity relation of coordinate frames was obtained in [2]. This method was applied to manipulate a multi-fingered robot hand in [3]. The challenges in multi-fingered robotic hands has attracted the attention of many researchers [3 – 13]. In most of the cases, authors examined the situation in which the frictional forces are large enough to prevent the object from slipping on fingers. The conditions required for the fingertips to hold the object without slipping were examined by taking the friction effect into account. The fingertips must be able to roll and/or slide over the object surface in order to achieve the desired position without breaking and re-establishing the contacts [1, 6, 14 – 16]. Contact points of the object and fingers may roll and/or slide. Therefore, rolling and sliding contact is an important issue that must be handled by multi-fingered hands. Although the Euclidean metric is commonly used, generalized metrics might be more suitable in future applications. To this purpose, we study the sliding and rolling motion by using a generalized metric that contains the Euclidean metric as special case.

In [17], authors investigated the velocity and acceleration equations for the contact between two 3-dimensional bodies by using the Christoffel symbols and fundamental forms of the associated surfaces. By using a different approach, kinematic equations similar to Montana's work (see [2]) was provided in [18]. In particular, the authors investigated a mathematical model of rolling between regular surfaces by using the principal curvatures of the surfaces, and they provided a constructive controllability algorithm for planning rolling motions for dexterous robot hands. Also, the authors developed Montana's classical contact kinematic equations using nonorthogonal object parameterizations in [19].

As the rolling motion and sliding motion are independent, the authors used the moving-frame method to give a geometric approach of this motion in [20 – 22]. (See [23, 24] for details of the moving-frame method.) In particular, they derived the system of equations for the velocity. The solutions to this system give the angular and linear velocities of an arbitrary point.

A new mathematical model of the inverse kinematics of the robotic-hand by using the singular value decomposition was obtained in [25]. In particular, the analytical solutions for the inverse kinematics was presented for the first time in that paper. A general approach for the kinematics of a sphere was presented in [26].

There are also several applications of this motion in the Minkowski space. For instance, a one-parameter Lorentzian spherical motion was studied in [27]. The inverse kinematic equations of spin-rolling motion without sliding a timelike surface on another timelike surface with the timelike velocity vector was studied in [28] in which various characterizations of spinning-rolling motion of the surfaces were given. Some other applications can be found in [29 – 36].

In kinematics studies, the moving-frame method is useful in investigating the kinematics of the contact of surfaces. Differential geometric properties of curves and surfaces are closely related to the concept of curvature (see [37]). These curvatures depend on the Darboux frame defined on the curve and surface. The Darboux frame is used to investigate the kinematics of the contact of objects on each other such as sliding-rolling-spinning. Velocity equations are given by using the curvatures obtained from derivative formulas of this moving-frame. In this aspect, our study is important. By defining the generalized Darboux frame, we give the kinematics of the sliding-rolling motion in a unified form. Hence, many of the studies mentioned above are a special case of this form. As an example, we study the kinematics of the sliding-rolling motion in semi-Euclidean space and show that L. Cui and J. S. Dai's work is a special case of our form.

In the present paper, we obtain kinematic equations when two objects maintain sliding-rolling contact in the semi-Euclidean 3-space $\mathbb{R}^3_\varepsilon$, $\varepsilon \in \{0,1\}$. We derive the velocities of the curve that is adjoint to a general surface. Then we present the fixed point conditions by using the Darboux frame. This approach is applied to the kinematics of two objects keeping sliding-rolling contact in this space. Then we give the angular and translational velocities of an arbitrary point of the moving surface on the fixed surface using the Darboux frame equations. We also investigate the rolling-sliding motion of the unit disc on the Lorentzian plane. Moreover, we apply the proposed approach to general surfaces in semi-Euclidean spaces.

As a result, in our study, we examine the sliding-rolling motion of two surfaces in both Euclidean and pseudo-Euclidean spaces. Our methodology is rooted in the application of the Darboux frame within these metrics. This approach enables us to derive kinematic equations, which we then apply to typical surface scenarios, including spacelike and timelike cases. The paper is enriched with visually informative illustrations, showcasing the motion of a hyperbolic cap as it rolls across the de Sitter space.

2. Preliminaries. Let $\varepsilon \in \{0,1\}$. Consider the 3-dimensional semi-Euclidean space $\mathbb{R}^3_\varepsilon$, defined as the vector space $\mathbb{R}^3$ equipped with the semi-Riemannian metric

$$g(\mathbf{v},\boldsymbol{\omega}) = (-\varepsilon_4)v_1\omega_1 + v_2\omega_2 + v_3\omega_3\,, \quad \varepsilon_4 = (-1)^{\varepsilon+1},$$

where $\mathbf{v} = (v_1, v_2, v_3)$, $\boldsymbol{\omega} = (\omega_1, \omega_2, \omega_3) \in \mathbb{R}^3_\varepsilon$. If $\varepsilon_4 = 1$, then we have three types of vectors according to their causal characters. Namely, $\mathbf{v}$ is said to be spacelike if $g(\mathbf{v},\mathbf{v}) = \mathbf{1}$, timelike if $g(\mathbf{v},\mathbf{v}) = -\mathbf{1}$ and lightlike (null) if $g(\mathbf{v},\mathbf{v}) = \mathbf{0}$ with $\mathbf{v} \neq \mathbf{0}$. A curve γ in $\mathbb{R}^3_\varepsilon$ is called spacelike (resp., timelike, lightlike) if all of its velocities are spacelike (resp., timelike, lightlike). A surface M said to be spacelike (resp., timelike, lightlike) if the unit normal vector of M is timelike (resp., spacelike, lightlike). If $\varepsilon_4 = -1$ then the vector $\mathbf{v}$, the curve γ and the surface M have a single causal character in the Euclidean sense.

The cross product of two vectors $\mathbf{u}, \mathbf{v} \in \mathbb{R}^{\mathbf{3}}_\varepsilon$ is defined as

$$\mathbf{u} \times \mathbf{v} = -\varepsilon_{\mathbf{4}}(\mathbf{u_2 v_3} - \mathbf{u_3 v_2})\mathbf{e_1} + (\mathbf{v_1 u_3} - \mathbf{v_3 u_1})\mathbf{e_2} + (\mathbf{u_1 v_2} - \mathbf{u_2 v_1})\mathbf{e_3}\,,$$

where $\mathbf{u} = (\mathbf{u_1}, \mathbf{u_2}, \mathbf{u_3})$, $\mathbf{v} = (\mathbf{v_1}, \mathbf{v_2}, \mathbf{v_3})$.

There exists an orthonormal Darboux frame $\{\mathbf{e_1}, \mathbf{e_2}, \mathbf{e_3}\}$ along the curve γ on the surface M. Here, $\mathbf{e_1} = \dfrac{\mathbf{d}\gamma}{\mathbf{ds}} = \gamma'$ is a tangent vector of γ, s denotes the arc-length of the curve, and $\mathbf{e_3}$ is unit normal vector of the surface M. The vector $\mathbf{e_2}$ is obtained by $\mathbf{e_2} = \mathbf{e_3} \times \mathbf{e_1}$. All together, they satisfy the following equation (see [23] for the Euclidean situation):

$$\begin{bmatrix}\mathbf{e_1'}\\ \mathbf{e_2'}\\ \mathbf{e_3'}\end{bmatrix} = \begin{bmatrix}0 & k_g & \varepsilon_3 k_n\\ \varepsilon_2 k_g & 0 & \varepsilon_1 \tau_g\\ \varepsilon_4 k_n & \varepsilon_4 \tau_g & 0\end{bmatrix}\begin{bmatrix}\mathbf{e_1}\\ \mathbf{e_2}\\ \mathbf{e_3}\end{bmatrix}. \tag{1}$$

Here, $g(\mathbf{e_1},\mathbf{e_1}) = \varepsilon_1,\ g(\mathbf{e_2},\mathbf{e_2}) = \varepsilon_2,\ g(\mathbf{e_3},\mathbf{e_3}) = \varepsilon_3,\ k_g = \varepsilon_2 g(\mathbf{e_1'},\mathbf{e_2}),\ k_n = g(\mathbf{e_1'},\mathbf{e_3}),\ \tau_g = \varepsilon_1\varepsilon_3 g(\mathbf{e_2'},\mathbf{e_3})$. In these formulas $k_g = \kappa\mathcal{C}(\theta)$, $k_n = \kappa\mathcal{S}(\theta)$, $\tau_g = \tau + \theta'$ where θ is the angle function between the normal and binormal vector field of γ. The equalities $C'(\theta) = \varepsilon_2 S(\theta),\ \mathcal{S}'(\theta) = C(\theta)$ and $C^2(\theta) - \varepsilon_2 S^2(\theta) = 1$ hold, where κ and τ are the curvature and torsion of γ.

If M is a timelike surface and γ is a timelike curve, then

$$\mathcal{C}(\theta) = \cosh\theta,\ \mathcal{S}(\theta) = \sinh\theta.$$

If both of M and γ are timelike (resp. spacelike), or if M and γ are in the Euclidean space, then

$$\mathcal{C}(\theta) = \cos\theta,\ \mathcal{S}(\theta) = \sin\theta.$$

The following are the special cases:

(a) If M is spacelike, then γ on M is spacelike and $\varepsilon_1 = 1,\ \varepsilon_2 = -1,\ \varepsilon_3 = 1,\ \varepsilon_4 = 1$.

(b) If M is a timelike and γ on M is spacelike, then $\varepsilon_1 = 1,\ \varepsilon_2 = 1,\ \varepsilon_3 = -1,\ \varepsilon_4 = 1$.

(c) If M is a timelike and γ on M is timelike, then $\varepsilon_1 = -1,\ \varepsilon_2 = 1,\ \varepsilon_3 = 1,\ \varepsilon_4 = 1$.

(d) If M is in the Euclidean space and γ is on M, then $\varepsilon_1 = 1,\ \varepsilon_2 = -1,\ \varepsilon_3 = 1,\ \varepsilon_4 = -1$.

3. An adjoint approximation to a general surface in semi-Euclidean space $\mathbb{R}^3_\varepsilon$. This paper gives a generalization for the adjoint approach to a general surface M. A point K traces a curve α_K on M, and a frame $\{K; \mathbf{e_1}, \mathbf{e_2}, \mathbf{e_3}\}$ moves with K. The moving Darboux frame equations are given as follows:

$$\frac{d}{ds}\begin{bmatrix}\mathbf{e_1}\\ \mathbf{e_2}\\ \mathbf{e_3}\end{bmatrix} = \begin{bmatrix}0 & k_g & \varepsilon_3 k_n\\ \varepsilon_2 k_g & 0 & \varepsilon_1 \tau_g\\ \varepsilon_4 k_n & \varepsilon_4 \tau_g & 0\end{bmatrix}\begin{bmatrix}\mathbf{e_1}\\ \mathbf{e_2}\\ \mathbf{e_3}\end{bmatrix}.$$

Here, $\mathbf{e_1}$ and $\mathbf{e_3}$ are the tangent vector of the curve and normal vector of the surface M at K, respectively. Also, $\dfrac{dr_{OK}}{ds} = e_1$, $g(\mathbf{e_1},\mathbf{e_1}) = \varepsilon_1$, $g(\mathbf{e_2},\mathbf{e_2}) = \varepsilon_2$, $g(\mathbf{e_3},\mathbf{e_3}) = \varepsilon_3$, and $\mathbf{r_{OK}}$ represents the vector from O to K according to the fixed frame $\{O; \mathbf{i}, \mathbf{j}, \mathbf{k}\}$, and s denotes the arc-length of the curve. If M is a spacelike or timelike surface in Minkowski 3-space, then $\varepsilon_4 = 1$. If M is a surface in Euclidean 3-space, then $\varepsilon_4 = -1$. The symbols τ_g, k_n and k_g show the geodesic torsion, normal curvature, and geodesic curvature of α_K, respectively. The curve α_P is determined by the point P according to $\{O; \mathbf{i}, \mathbf{j}, \mathbf{k}\}$ frame. The curve α_P is called adjoint curve of the curve α_K. Therefore, the vector equality of the curve α_P according to the frame $\{O; \mathbf{i}, \mathbf{j}, \mathbf{k}\}$ can be written as

$$\mathbf{r_{OP}} = \mathbf{r_{OK}} + p_1\mathbf{e_1} + p_2\mathbf{e_2} + p_3\mathbf{e_3},$$

where (p_1, p_2, p_3) are the coordinates of P according to the frame $\{K; \mathbf{e_1}, \mathbf{e_2}, \mathbf{e_3}\}$, and $\mathbf{r_{OP}}$ is the vector from O to P according to the frame $\{O; \mathbf{i}, \mathbf{j}, \mathbf{k}\}$. If we differentiate the vector $\mathbf{r_{OP}}$ with respect to the parameter s of the locus α_K, then we obtain the following equation, by using the Darboux frame equations:

$$\frac{d\mathbf{r}_{\mathbf{OP}}}{ds} = A_1\mathbf{e_1} + A_2\mathbf{e_2} + A_3\mathbf{e_3}, \tag{2}$$

where

$$\begin{aligned} A_1 &= 1 + \frac{dp_1}{ds} + \varepsilon_2 k_g p_2 + \varepsilon_4 k_n p_3, \\ A_2 &= \frac{dp_2}{ds} + k_g p_1 + \varepsilon_4 \tau_g p_3, \\ A_3 &= \frac{dp_3}{ds} + \varepsilon_3 k_n p_1 + \varepsilon_1 \tau_g p_2. \end{aligned} \tag{3}$$

The equation in (3) is called the adjoint equation.

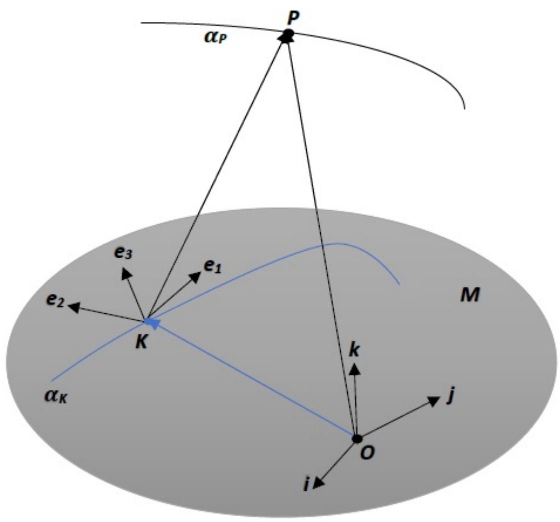

Fig. 1. The curve α_P adjoint to the curve α_K on the surface M.

In Fig. 1, P is a fixed point according to the fixed frame $\{O;\mathbf{i},\mathbf{j},\mathbf{k}\}$ and K is a moving point on the surface M according to the moving frame $\{K;\mathbf{e_1},\mathbf{e_2},\mathbf{e_3}\}$. The vectors $\mathbf{KP}$ and $\mathbf{OK}$ change in time, however their sum, $\mathbf{OP}$, remains constant. Then the points K draw a curve α_K, and the points P draw a curve α_P. The curve α_P is adjoint to the curve α_K on the surface M. Therefore, P is a fixed point according to the frame $\{O;\mathbf{i},\mathbf{j},\mathbf{k}\}$, the vector $\dfrac{d\mathbf{r}_{\mathbf{OP}}}{ds}$ vanishes. Hence, all of A_1, A_2 and A_3 are equal to zero. This gives

$$\begin{aligned} \frac{dp_1}{ds} &= -\varepsilon_2 k_g p_2 - \varepsilon_4 k_n p_3 - 1, \\ \frac{dp_2}{ds} &= -k_g p_1 - \varepsilon_4 \tau_g p_3, \\ \frac{dp_3}{ds} &= -\varepsilon_3 k_n p_1 - \varepsilon_1 \tau_g p_2. \end{aligned} \tag{4}$$

The equation in (4) is called the fixed point condition of the fixed point P.

4. Kinematics properties of contact loci of the sliding-rolling motion. A regular curve can be parameterized by its arc-length parameter. Therefore, we can parametrize contact loci curves according to their arc-length parameters. In [21], the parameters for the investigation of geometric properties of the motion were chosen as the arc lengths of the contact loci. In this sense, we extend the work [21] to semi-Euclidean space $\mathbb{R}^3_\varepsilon$, where $\varepsilon \in \{0,1\}$. In this section, we obtain a generalization of this movement using a general framework that includes both Minkowski and Euclidean spaces.

Next, we give two cases related to the adjoint curves of the fixed and moving surfaces in $\mathbb{R}^3_\varepsilon$.

Consider a fixed surface M. Let M^* be the moving surface such that they keep sliding-rolling contact at any movement. We denote the frame on M by $\{O;\mathbf{i},\mathbf{j},\mathbf{k}\}$, the frame on M^* by $\{O^*;\mathbf{i}^*,\mathbf{j}^*,\mathbf{k}^*\}$, the contact loci on M by α, and the contact loci the M^* by α^*. The curve α^* on M^* is only generated via the rolling motion and the curve α on M is obtained by both sliding and rolling motions of the contact points K and K^* on M and M^*, respectively. The points K and K^* coincide as long as M and M^* maintain a point contact. Let two right-handed orthonormal Darboux moving frames related to the contact loci α and α^* be represented by $\{K;\mathbf{e_1},\mathbf{e_2},\mathbf{e_3}\}$ and $\{K;\mathbf{e_1^*},\mathbf{e_2^*},\mathbf{e_3^*}\}$, respectively. Here, $\mathbf{e_1}$ and $\mathbf{e_1^*}$ are the unit tangent vectors of the related curves, and $\mathbf{e_3}$ and $\mathbf{e_3^*}$ are the unit normal vectors of the related surfaces. Directions of the sliding and rolling motions are different in general. Therefore, there is an angle θ between $\mathbf{e_1}$ and $\mathbf{e_1^*}$ (see [21] and Fig. 2).

Case 1. Suppose that P is an arbitrary point on M^*. The position vector r_{O^*P} according to the frame $\{O^*;\mathbf{i}^*,\mathbf{j}^*,\mathbf{k}^*\}$ can be written as

$$\mathbf{r_{O^*P}} = \mathbf{r_{O^*K}} + p_1^*\mathbf{e_1^*} + p_2^*\mathbf{e_2^*} + p_3^*\mathbf{e_3^*}, \tag{5}$$

where (p_1^*,p_2^*,p_3^*) are the coordinates of P according to the frame $\{K;\mathbf{e_1^*},\mathbf{e_2^*},\mathbf{e_3^*}\}$. By using the fixed point condition in Eq. (4), we get

$$\begin{aligned}
\frac{dp_1^*}{ds^*} &= -\varepsilon_2 k_g^* p_2^* - \varepsilon_4 k_n^* p_3^* - 1,\\
\frac{dp_2^*}{ds^*} &= -k_g^* p_1^* - \varepsilon_4 \tau_g^* p_3^*,\\
\frac{dp_3^*}{ds^*} &= -\varepsilon_3 k_n^* p_1^* - \varepsilon_1 \tau_g^* p_2^*,
\end{aligned}$$

where k_g^*, k_n^* and τ_g^* are the geodesic curvature, the normal curvature, and the geodesic torsion of the frame $\{K;\mathbf{e_1^*},\mathbf{e_2^*},\mathbf{e_3^*}\}$, respectively. The notion s^* represents the arc-length of the curve α^*. The parameter s^* is the distance of the contact point M traveling due to rolling motion.

Case 2. The point P generates curve α_P during the rolling-sliding motion of the surface M^* on the fixed surface M. Since the curve α_P is tangent to the contact locus α, equation (3) in the adjoint system yields the velocity of α_P, as outlined in equations (2) and (3).

4.1. The connection with the points p and p*. The frame $\{K;\mathbf{e_1^*},\mathbf{e_2^*},\mathbf{e_3^*}\}$ is achieved via rotating the frame $\{K;\mathbf{e_1},\mathbf{e_2},\mathbf{e_3}\}$ by an angle of θ about the $\mathbf{e_3}$ axis, as shown in Fig. 2.

Then we have

$$\begin{aligned}
\mathbf{e_1^*} &= \mathcal{C}(\theta)\mathbf{e_1} - \varepsilon_2\mathcal{S}(\theta)\mathbf{e_2},\\
\mathbf{e_2^*} &= -\mathcal{S}(\theta)\mathbf{e_1} + \mathcal{C}(\theta)\mathbf{e_2},\\
\mathbf{e_3^*} &= \mathbf{e_3}.
\end{aligned}$$

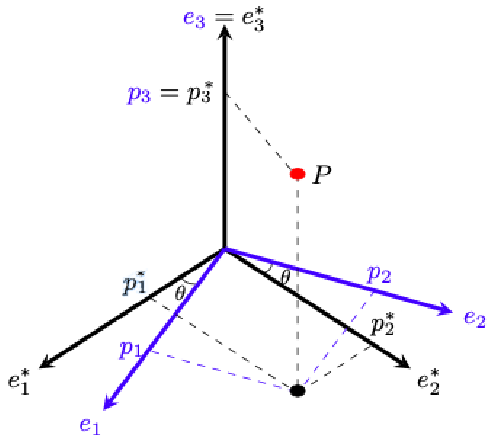

Fig. 2. The relations of two frames.

If $\varepsilon_2 = -1$, then M is a spacelike surface and the plane $sp\{\mathbf{e_1}, \mathbf{e_2}\}$ is a spacelike plane. This gives

$$\mathcal{C}(\theta) = \cos\theta, \quad \mathcal{S}(\theta) = \sin\theta.$$

If $\varepsilon_2 = 1$, then M is a timelike surface and the plane $sp\{\mathbf{e_1}, \mathbf{e_2}\}$ is a timelike plane. This gives

$$\mathcal{C}(\theta) = \cosh\theta, \quad \mathcal{S}(\theta) = \sinh\theta.$$

Here, $\mathcal{C}'(\theta) = \varepsilon_2 \mathcal{S}(\theta)$, $\mathcal{S}'(\theta) = \mathcal{C}(\theta)$ and $\mathcal{C}^2(\theta) - \varepsilon_2\mathcal{S}^2(\theta) = 1$.

In particular, the coordinates (p_1, p_2, p_3) and (p_1^*, p_2^*, p_3^*) are related by the following equations:

$$\begin{aligned} p_1 &= \mathcal{C}(\theta)p_1^* + \varepsilon_2\mathcal{S}(\theta)p_2^*, \\ p_2 &= \mathcal{S}(\theta)p_1^* + \mathcal{C}(\theta)p_2^*, \\ p_3 &= p_3^*. \end{aligned} \tag{6}$$

Differentiating Eq. (6) with respect to the arc-length s of the contact locus α and using the fix point condition, we obtain

$$\begin{aligned} \frac{dp_1}{ds} &= \lambda\left[\varepsilon_2\left(\frac{d\theta}{ds^*} - k_g^*\right)p_2 - \varepsilon_4\big(k_n^*\mathcal{C}(\theta) + \varepsilon_2\tau_g^*\mathcal{S}(\theta)\big)p_3 - \mathcal{C}(\theta)\right], \\ \frac{dp_2}{ds} &= \lambda\left[\varepsilon_2\left(\frac{d\theta}{ds^*} - k_g^*\right)p_1 - \varepsilon_4\big(k_n^*\mathcal{S}(\theta) + \tau_g^*\mathcal{C}(\theta)\big)p_3 - \mathcal{S}(\theta)\right], \\ \frac{dp_3}{ds} &= \lambda\Big[\Big(-\varepsilon_3\mathcal{C}(\theta)k_n^* - \varepsilon_1\varepsilon_2\tau_g^*\mathcal{S}(\theta)\Big)p_1 + \Big(-\varepsilon_3\mathcal{S}(\theta)k_n^* - \varepsilon_1\tau_g^*\mathcal{C}(\theta)\Big)p_2\Big], \end{aligned} \tag{7}$$

where λ is the ratio of rolling rate ds^* to the rolling-sliding rate ds.

We now use the above formulas to define the geometric velocity of P. By using Eqs. (5) and (7), the geometric velocity of the point P is calculated as

$$\frac{\mathbf{dr_{OP}}}{ds} = A_1\mathbf{e_1} + A_2\mathbf{e_2} + A_3\mathbf{e_3},$$

where

$$A_1 = 1 - \lambda\mathcal{C}(\theta) + \left[\lambda\left(\frac{d\theta}{ds^*} - k_g^*\right) + k_g\right]\varepsilon_2 p_2 + \left[\lambda\Big(- k_n^*\mathcal{C}(\theta) - \varepsilon_2\tau_g^*\mathcal{S}(\theta)\Big) + k_n\right]\varepsilon_4 p_3,$$

$$A_2 = -\lambda\mathcal{S}(\theta) + \left[\lambda\left(\frac{d\theta}{ds^*} - k_g^*\right) + k_g\right]p_1 + \left[\lambda\Big(- k_n^*\mathcal{S}(\theta) - \tau_g^*\mathcal{C}(\theta)\Big) + \tau_g\right]\varepsilon_4 p_3,$$

$$A_3 = \left[\lambda\Big(- \varepsilon_3\mathcal{C}(\theta)k_n^* - \varepsilon_1\varepsilon_2\tau_g^*\mathcal{S}(\theta)\Big) + \varepsilon_3 k_n\right]p_1 + \left[\lambda\Big(- \varepsilon_3\mathcal{S}(\theta)k_n^* - \varepsilon_1\tau_g^*\mathcal{C}(\theta)\Big) + \varepsilon_1\tau_g\right]p_2.$$

Hence, we obtained the geometric velocity (according to the arc-length parameter) of the contact locus α at an arbitrary point P in the frame $\{O; \mathbf{i}, \mathbf{j}, \mathbf{k}\}$.

5. The general form for the DOFs of moving surface in $\mathbb{R}^3_\varepsilon$. In three dimensional spaces, an object consists of six DOFs. Namely, it has three translational DOFs and three rotational DOFs. However, while two objects maintain the rolling-sliding contact, one translational DOFs is reduced in the direction parallel to the normal vector at the point of contact. Thus, the moving surface has two translational DOFs and three rotational DOFs. The five DOFs according to the frame $\{K; \mathbf{e_1}, \mathbf{e_2}, \mathbf{e_3}\}$ are given as follows:

$$\mathbf{v} = v_1\mathbf{e_1} + v_2\mathbf{e_2},$$

$$\boldsymbol{\omega} = \omega_1\mathbf{e_1} + \omega_2\mathbf{e_2} + \omega_3\mathbf{e_3}.$$

Here, $\mathbf{v}$ is the translational velocity and ω is the rotational velocity.

These velocities can be expressed in two forms as follows. The geometric velocity in Eq. (2) gives the first form as

$$\mathbf{v_P} = \frac{d\mathbf{r_{OP}}}{dt} = \frac{ds}{dt}\frac{d\mathbf{r_{OP}}}{ds} = \sigma(A_1\mathbf{e_1} + A_2\mathbf{e_2} + A_3\mathbf{e_3}),$$

where the parameter t is the time parameter in the physical sense, s is the arc-length of the curve, and $\sigma = ds/dt$ denotes the rolling-sliding rate. The second form is given as

$$\begin{aligned}
\mathbf{v_{OP}} &= \mathbf{v} + \boldsymbol{\omega}\times\mathbf{r_{MP}} \\
&= \mathbf{v} + (\omega_1\mathbf{e_1} + \omega_2\mathbf{e_2} + \omega_3\mathbf{e_3})\times(p_1\mathbf{e_1} + p_2\mathbf{e_2} + p_3\mathbf{e_3}) \\
&= \big(v_1 - \varepsilon_4(p_3\omega_2 - p_2\omega_3)\big)\mathbf{e_1} + (v_2 + p_1\omega_3 - p_3\omega_1)\mathbf{e_2} + (p_2\omega_1 - p_1\omega_2)\mathbf{e_3}.
\end{aligned}$$

Since these two forms are equal we obtain the following equations:

$$\begin{aligned}
v_1 - \varepsilon_4(p_3\omega_2 - p_2\omega_3) &= \sigma\Big(1 - \lambda\mathcal{C}(\theta) + \Big[\lambda\Big(\frac{d\theta}{ds^*} - k_g^*\Big) + k_g\Big]\varepsilon_2 p_2 \\
&\quad + \Big[\lambda\big(- k_n^*\mathcal{C}(\theta) - \varepsilon_2\tau_g^*\mathcal{S}(\theta)\big) + k_n\Big]\varepsilon_4 p_3\Big), \\
v_2 + p_1\omega_3 - p_3\omega_1 &= \sigma\Big(- \lambda\mathcal{S}(\theta) + \Big[\lambda\Big(\frac{d\theta}{ds^*} - k_g^*\Big) + k_g\Big]p_1 \\
&\quad + \big[\lambda\big(- \varepsilon_4 k_n^*\mathcal{S}(\theta) - \varepsilon_4\tau_g^*\mathcal{C}(\theta)\big) + \varepsilon_4\tau_g\big]p_3\Big), \\
p_2\omega_1 - p_1\omega_2 &= \sigma\bigg(\Big[\lambda\big(- \varepsilon_3\mathcal{C}(\theta)k_n^* - \varepsilon_1\varepsilon_2\tau_g^*\mathcal{S}(\theta)\big) + \varepsilon_3 k_n\Big]p_1 \\
&\quad + \Big[\lambda\big(- \varepsilon_3\mathcal{S}(\theta)k_n^* - \varepsilon_1\tau_g^*\mathcal{C}(\theta)\big) + \varepsilon_1\tau_g\Big]p_2\bigg).
\end{aligned} \tag{8}$$

The coordinates p_1, p_2, p_3 of P take arbitrary values as P is an arbitrary point. The coefficients of p_1, p_2, p_3 must be equal on both sides of each equation in Eqs. (8), respectively. If we equate such coefficients on both sides of Eqs. (8), the first equation gives

$$v_1 = \sigma\big(1 - \lambda\mathcal{C}(\theta)\big),$$

$$\omega_2 = \sigma\Big[\lambda\big(k_n^*\mathcal{C}(\theta) + \varepsilon_2\tau_g^*\mathcal{S}(\theta)\big) - k_n)\Big],$$

$$\omega_3 = \varepsilon_4\sigma\Big[\lambda\varepsilon_2\Big(\frac{d\theta}{ds^*} - k_g^*\Big) + \varepsilon_2 k_g\Big],$$

while the second equation gives

$$v_2 = \sigma\big(-\lambda\mathcal{S}(\theta)\big),$$

$$\omega_1 = \sigma\Big[\lambda\big(\varepsilon_4 k_n^*\mathcal{S}(\theta) + \varepsilon_4\tau_g^*\mathcal{C}(\theta)\big) - \varepsilon_4\tau_g\Big],$$

$$\omega_3 = \sigma\Big[\lambda\Big(\frac{d\theta}{ds^*} - k_g^*\Big) + k_g\Big].$$

Using the third equation, we can write

$$\omega_1 = \sigma\Big[\lambda\big(-\varepsilon_3\mathcal{S}(\theta)k_n^* - \varepsilon_1\tau_g^*\mathcal{C}(\theta)\big) + \varepsilon_1\tau_g\Big],$$

$$\omega_2 = \sigma\Big[\lambda\big(\varepsilon_3\mathcal{C}(\theta)k_n^* + \varepsilon_1\varepsilon_2\tau_g^*\mathcal{S}(\theta)\big) - \varepsilon_3 k_n\Big].$$

In the next section, we provide two special cases of the characterizations obtained in above sections. The first case is given in Subsection 6.1, where we describe the sliding-rolling loci kinematics in the Minkowski 3-space. The second case is given in Subsection 6.2, where we obtain the sliding-rolling loci kinematics in the Euclidean space.

6. Special cases for the velocity of moving surfaces in $\mathbb{R}^3_\varepsilon$. In this section, we demonstrate the velocity of moving surfaces in three special cases.

6.1. The velocity of moving surfaces in the Minkowski space $\mathbb{R}^3_1$.

Case 1. If M is a spacelike surface, then γ can be a spacelike curve. In such case, $\varepsilon_1 = \varepsilon_3 = \varepsilon_4 = 1$ and $\varepsilon_2 = -1$. This provides the following translational and angular velocities of M:

$$\mathbf{v} = \sigma(1 - \lambda\cos\theta)\mathbf{e_1} - \sigma\lambda\sin\theta\mathbf{e_2},$$

$$\boldsymbol{\omega} = \sigma\big(\lambda(k_n^*\cos\theta - \tau_g^*\sin\theta) - k_n\big)\mathbf{e_2}.$$

Here, $\lambda k_n^*\sin\theta + \lambda\tau_g^*\cos\theta - \tau_g = 0$ and $-\lambda k_g^* + \lambda\dfrac{d\theta}{ds^*} + k_g = 0$.

Case 2. If M is a timelike surface, then γ can be a spacelike or timelike curve. If γ is spacelike, then $\varepsilon_1 = \varepsilon_2 = \varepsilon_4 = 1$, $\varepsilon_3 = -1$. This provides the following velocities of the moving surface:

$$\mathbf{v} = \sigma(1 - \lambda\cosh\theta)\mathbf{e_1} - \sigma\lambda\sinh\theta\mathbf{e_2},$$

$$\boldsymbol{\omega} = \sigma(\lambda k_n^*\sinh\theta)\mathbf{e_1} + \sigma(\lambda\tau_g^*\sinh\theta)\mathbf{e_2} + \sigma\left(\lambda\left(-k_g^* + \frac{d\theta}{ds^*}\right) + k_g\right)\mathbf{e_3}.$$

Here, $\lambda\tau_g^*\cosh\theta - \tau_g = 0$ and $\lambda k_n^*\cosh\theta - k_n = 0$.

If γ is timelike, then $\varepsilon_2 = \varepsilon_3 = \varepsilon_4 = 1,\ \varepsilon_1 = -1$. This gives the velocities of M as follows:

$$\begin{aligned} \mathbf{v} &= \sigma(1-\lambda\cosh\theta)\mathbf{e_1} - \sigma\lambda(\sinh\theta)\mathbf{e_2}, \\ \boldsymbol{\omega} &= \sigma\big(\lambda\tau_g^*\cosh\theta - \tau_g\big)\mathbf{e_1} + \sigma\big(\lambda(\cosh\theta)k_n^* - k_n\big)\mathbf{e_2} + \sigma\left(\lambda\left(-k_g^* + \frac{d\theta}{ds^*}\right) + k_g\right)\mathbf{e_3}. \end{aligned} \tag{9}$$

Here, $\lambda(\sinh\theta)k_n^* = 0$ and $\lambda\tau_g^*\sinh\theta = 0$.

6.2. The velocity of moving surfaces in the Euclidean 3-space $\mathbb{R}^3$. The equations and results that we obtain in this subsection are the same as those of [21]. Therefore, this study is a generalization of the work [21].

If M is a surface in the Euclidean 3-space, then we have $\varepsilon_1 = \varepsilon_3 = 1,\ \varepsilon_2 = \varepsilon_4 = -1$ leading to the following velocities of M:

$$\begin{aligned} v_1 &= \sigma\big(1-\lambda\mathcal{C}(\theta)\big), \\ \omega_2 &= \sigma\Big(\lambda\big(k_n^*\mathcal{C}(\theta) - \tau_g^*\mathcal{S}(\theta)\big) - k_n\Big), \\ \omega_3 &= \sigma\left(\lambda\left(\frac{d\theta}{ds^*} - k_g^*\right) + k_g\right). \end{aligned}$$

The second equation gives

$$\begin{aligned} v_2 &= \sigma\big(-\lambda\mathcal{S}(\theta)\big), \\ \omega_1 &= \sigma\Big(\lambda\big(-k_n^*\mathcal{S}(\theta) - \tau_g^*\mathcal{C}(\theta)\big) + \tau_g\Big), \\ \omega_3 &= \sigma\left(\lambda\left(\frac{d\theta}{ds^*} - k_g^*\right) + k_g\right). \end{aligned}$$

The third equation implies

$$\begin{aligned} \omega_1 &= \sigma\Big(\lambda\big(-\mathcal{S}(\theta)k_n^* - \tau_g^*\mathcal{C}(\theta)\big) + \tau_g\Big), \\ \omega_2 &= \sigma\Big(\lambda\big(\mathcal{C}(\theta)k_n^* - \tau_g^*\mathcal{S}(\theta)\big) - k_n\Big). \end{aligned}$$

Therefore, the velocities of M are calculated as follows:

$$\begin{aligned} v &= \sigma(1-\lambda\cos\theta)e_1 - \sigma\lambda\sin\theta e_2, \\ \omega_1 &= \sigma\big(\lambda(-\sin\theta k_n^* - \tau_g^*\cos\theta) + \tau_g\big)e_1 \\ &\quad + \sigma\big(\lambda(\cos\theta k_n^* - \tau_g^*\sin\theta) - k_n\big)e_2 \\ &\quad + \sigma\left(\lambda\left(\frac{d\theta}{ds^*} - k_g^*\right) + k_g\right)e_3. \end{aligned}$$

In the following section, we present various examples to describe the sliding-rolling loci.

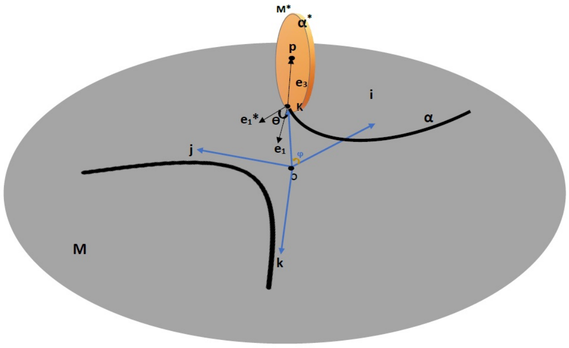

Fig. 3. Rolling-sliding motion of the unit disc along a Lorentzian circle.

7. Example of the sliding-rolling loci in the Minkowski 3-space $\mathbb{R}^3_1$. Consider the unit disc (denoted by M^*) that maintains a sliding-rolling contact with the plane M. Then the contact loci is a Lorentzian circle α on the plane M, and the circle α^* on the disc. The angle between α^* and α at the contact point M is represented by φ. The notion σ denotes the rolling-sliding rate according to the arc-length of α, and λ represents the ratio of rolling rate ds^* to sliding-rolling rate ds. They are plotted in Fig. 3.

Let $\{K;\mathbf{e_1},\mathbf{e_2},\mathbf{e_3}\}$ be the frame on the contact loci α and $\{K;\mathbf{e_1^*},\mathbf{e_2^*},\mathbf{e_3^*}\}$ be the frame on the contact loci α^*. Here, $\mathbf{e_1}$ is the tangent vector of Lorentzian circle α, $\mathbf{e_3}$ is the normal vector of M, $\mathbf{e_1^*}$ is the tangent vector of α^*, and $\mathbf{e_3^*}$ is the normal of the circle, pointing the center of the disc.

Then the frame $\{K;\mathbf{e_1},\mathbf{e_2},\mathbf{e_3}\}$ satisfies

$$\frac{d}{ds}\begin{bmatrix}\mathbf{e_1}\\ \mathbf{e_2}\\ \mathbf{e_3}\end{bmatrix}=\begin{bmatrix}0 & \kappa & 0\\ -\kappa & 0 & 0\\ 0 & 0 & 0\end{bmatrix}\begin{bmatrix}\mathbf{e_1}\\ \mathbf{e_2}\\ \mathbf{e_3}\end{bmatrix}, \tag{10}$$

where κ is the curvature of α and s is the arc-length of α on M.

The frame $\{K;\mathbf{e_1^*},\mathbf{e_2^*},\mathbf{e_3^*}\}$ is given as

$$\frac{d}{ds}\begin{bmatrix}\mathbf{e_1^*}\\ \mathbf{e_2^*}\\ \mathbf{e_3^*}\end{bmatrix}=\begin{bmatrix}0 & 0 & \kappa^*\\ 0 & 0 & 0\\ -\kappa^* & 0 & 0\end{bmatrix}\begin{bmatrix}\mathbf{e_1^*}\\ \mathbf{e_2^*}\\ \mathbf{e_3^*}\end{bmatrix}, \tag{11}$$

where κ^* is the curvature of the unit Lorentzian circle α^* and it satisfies $\kappa^*=1$. Also, s^* is the arc-length of the curve α^* on M^*.

Using Eqs. (10) and (11) in equations (9), we calculate the velocities of the disc as follows:

$$\mathbf{v}=\sigma(1-\lambda\cosh\theta)\mathbf{e_1}-\sigma\lambda\sinh\theta\mathbf{e_2},$$

$$\boldsymbol{\omega}=\sigma\lambda\cosh\theta\mathbf{e_2}+\sigma^2\kappa\mathbf{e_3},\ \theta=0.$$

Here, σ is the sliding-rolling rate and λ is the ratio of the rolling rate ds^* to the sliding-rolling rate ds. Then the velocity of p is computed as

$$\mathbf{v}_p=\mathbf{v}+\boldsymbol{\omega}\times\mathbf{e_3}=\sigma(1-2\lambda)\mathbf{e_1}.$$

7.1. Numerical simulation. Let the contact locus α on M be a Lorentzian circle of curvature 0.25 with $\sigma = 1$ and $\lambda = 0.25$ as in Fig. 3.

Consider the fixed frame $\{O; \mathbf{i}, \mathbf{j}, \mathbf{k}\}$. Assume that the k-axis is perpendicular to the plane, as in Fig 2. Let the angle between the i-axis and **OK** be θ. Then, it can be verified that $\theta = s\kappa$ where $s = \sigma \dfrac{t}{4}$ is the arc-length parameter enclosed in the period of time t.

Then the vectors $\mathbf{e_1}$, e_2, and $\mathbf{e_3}$ according to the fixed frame $\{O; \mathbf{i}, \mathbf{j}, \mathbf{k}\}$ are

$$\mathbf{e_1} = \left[\sinh\frac{t}{4}, \cosh\frac{t}{4}, 0\right],$$

$$\mathbf{e_2} = \left[\cosh\frac{t}{4}, \sinh\frac{t}{4}, 0\right],$$

$$\mathbf{e_3} = [0, 0, -1].$$

The velocity components are plotted in Figs. 4, 5.

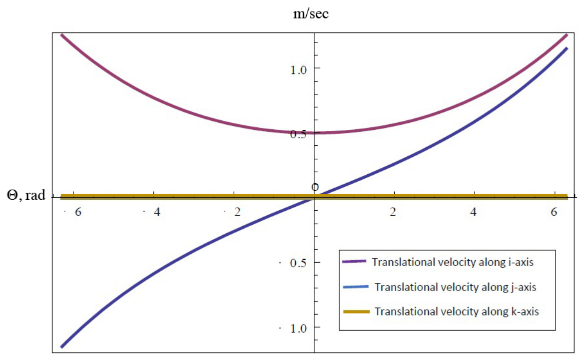

Fig. 4. Translational velocity components along $\mathbf{i}-, \mathbf{j}-, \mathbf{k}-$ axis.

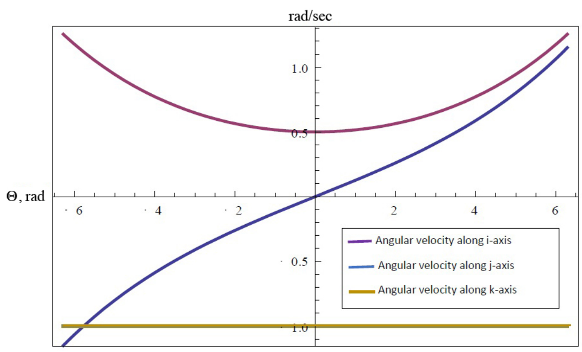

Fig. 5. Angular velocity components of the moving surface.

Consider the de Sitter space formed by rotating $\alpha(s) = \left(\dfrac{s^2}{2}, \dfrac{s^2}{2} - 1, s\right)$. Attach the moving frames $\{K; \mathbf{e_1}, \mathbf{e_2}, \mathbf{e_3}\}$ and $\{K; \mathbf{e_1^*}, \mathbf{e_2^*}, \mathbf{e_3^*}\}$ to the contact loci α and α^*, respectively. Here, $\mathbf{e_1}$ is the tangent vector of α, $\mathbf{e_3}$ is the upward normal vector of the de Sitter surface M, $\mathbf{e_1^*}$ is the tangent vector of the circle α^*, and $\mathbf{e_3^*}$ is the normal of the hyperbolic cap, pointing the hyperbolic cap center.

The moving frame equation related to the frame $\{K;\mathbf{e_1},\mathbf{e_2},\mathbf{e_3}\}$ is given as

$$\frac{d}{ds}\begin{bmatrix}\mathbf{e_1}\\ \mathbf{e_2}\\ \mathbf{e_3}\end{bmatrix}=\begin{bmatrix}0 & 1 & -1\\ 1 & 0 & 0\\ 1 & 0 & 0\end{bmatrix}\begin{bmatrix}\mathbf{e_1}\\ \mathbf{e_2}\\ \mathbf{e_3}\end{bmatrix}. \tag{12}$$

The moving Darboux frame equation related to the frame $\{K;\mathbf{e_1^*},\mathbf{e_2^*},\mathbf{e_3^*}\}$ is

$$\frac{d}{ds}\begin{bmatrix}\mathbf{e_1^*}\\ \mathbf{e_2^*}\\ \mathbf{e_3^*}\end{bmatrix}=\begin{bmatrix}0 & -\sqrt{2} & 1\\ \sqrt{2} & 0 & 0\\ 1 & 0 & 0\end{bmatrix}\begin{bmatrix}\mathbf{e_1^*}\\ \mathbf{e_2^*}\\ \mathbf{e_3^*}\end{bmatrix}. \tag{13}$$

Using Eqs. (12) and (13) in equations (9) the velocities of the hyperbolic cap on the de Sitter space are obtained as

$$\mathbf{v}=\sigma 2\mathbf{e_1}-\sigma\lambda\sqrt{\frac{1}{\lambda^2}-1}\mathbf{e_2},$$

$$\boldsymbol{\omega}=\sigma\left(-\lambda\sqrt{\frac{1}{\lambda^2}-1}\right)\mathbf{e_1}+\sigma(\lambda(\sqrt{2})+1)\mathbf{e_3}.$$

The motion of the hyperbolic cap on the fixed surface de Sitter space plotted in Fig. 6.

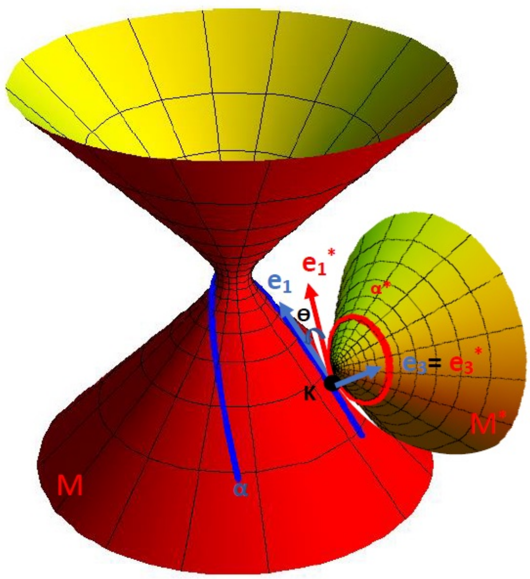

Fig. 6. The hyperbolic cap sliding-rolling on the de Sitter space.

8. Conclusion. When two objects maintain the sliding-rolling motion, the contact points trace a regular curve in the 3-dimensional space. The tangent, normal, and binormal vectors describe the kinematic and geometric properties of these motions. Types of these vectors affect this trajectory during the sliding-rolling motion. The time dimension also affects the trajectory. Therefore, for more general results, the sliding-rolling motion of these two objects should be investigated by taking the time dimension into account. In this article, we studied the effects of the time-dimension on the sliding-rolling motion of two objects. For this, we used the general Frenet frame given in Eq. (1) which ideally describes the time-dependent sliding-rolling motion. In other words, the generalized frame includes the Darboux frames of both Minkowski 3-space and Euclidean 3-space. By using the generalized frame that we defined in this study, we obtained the equations of sliding-rolling motion both in Lorentz – Minkowski and Euclidean spaces. Thus, our study includes the paper [21] in the Euclidean space as a special case. Moreover, the equations of motion of all surfaces with causal characters in the Lorentz – Minkowski space are also special cases of our characterization. For example, there are three spheres in the Lorentz – Minkowski space. They can be defined as a set of spacelike, timelike and lightlike unit vectors. If one of the two surfaces is a sphere, then there are three separate cases in the sliding-rolling movement of the two surfaces. As a result, the equations of the sliding-rolling motion for these different cases are special cases of our general equations. We believe that this metric and frame can be used for different equations of motion problems.

Conflict of interest. The authors declare that they have no potential conflict of interest in relation to the study in this paper.

Funding. The authors declare that no funds, grants, or other support were received during the preparation of this manuscript.

Author contributions. The author contributions are in accordance with the order of their names, with the 1st author contributing the most, followed by the 2nd author, and finally the 3rd author.

References

1. C. Cai, B. Roth, *On the spatial motion of rigid bodies with point contact*, in: IEEE Conference on Robotics and Automation (1987), p. 686 – 695.
2. D.J. Montana, *The kinematics of contact and grasp*, Int. J. Robot. Res., **7**, № 3, 17 – 32 (1988).
3. Z. Li, P. Hsu, S. Sastry, *Grasping and coordinated manipulation by a multi-fingered robot hand*, Int. J. Robot. Res., **8**, № 4, 33 – 50 (1989).
4. M. R. Cutkosky, *Robotic grasping and fine manipulation*, Kluwer Academic, Dordrecht (1985).
5. R. S. Fearing, *Simplified grasping and manipulation with dextrous robot hand*, IEEE J. Robot. Automat., **2**, № 4, 188 – 195 (1986).
6. J. R. Kerr, *An analysis of multi fingered hands*, PhD Dissertation, Stanford University (1984).
7. J. Kerr, B. Roth, *An analysis of multi fingered hands*, Int. J. Robot. Res., **4**, № 4, 3 – 17 (1986).
8. Y. Nakamura, K. Nagai, T. Yoshikawa, *Dynamics, stability in coordination of multiple robotic mechanisms*, Int. J. Robot. Res., **8**, № 2, 44 – 61 (1989).
9. E. Paljug, X. Yun, V. Kumar, *Control of rolling contacts in multi-arm manipulation*, IEEE Trans. Robot. Automat., **10**, № 4, 441 – 452 (1994).
10. G. P. Starr, *Experiments in assembly using a dextrous hand*, IEEE Trans. Robot. Automat., **6**, № 3, 342 – 347 (1990).
11. J. C. Trinkle, J. M. Abel, R. P. Paul, *An investigation of frictionless enveloping grasping in the plane*, Int. J. Robot. Res., **7**, № 3, 33 – 50 (1988).
12. J. C. Trinkle, *A quasi-static analysis of dextrous manipulation with sliding and rolling contacts*, in: Proceedings 1989 International Conference on Robotics and Automation, **2** (1989), p. 788 – 793.
13. M. Zribi, J. Chen, M. S. Mahmoud, *Coordination and control of multi-fingered robot hands with rolling and sliding contacts*, J. Intelligent and Robot. Systems, **24**, 125 – 149 (1999).
14. D. L. Brock, *Enhancing the dexterity of a robot hand using controlled slip*, in: Proceedings 1988 IEEE International Conference on Robotics and Automation, **1** (1988), p. 249 – 251.
15. R. C. Brost, *Automatic grasp planning in the presence of uncertainty*, Int. J. Robot. Res., **7**, № 1, 3 – 50 (1988).

16. C. Cai, B. Roth, *On the planar motion of a rigid body with point contact*, Mech. Mach. Theory, **21**, № 6, 453 – 466 (1986).
17. N. Sarkar, V. Kumar, X. Yun, *Velocity and acceleration equations for three-dimensional contact*, J. Appl. Mech., **63**, 974 – 984 (1996).
18. A. Marigo, A. Bicchi, *Rolling bodies with regular surface: controllability theory and application*, IEEE Trans. Automat. Control, **45**, 1586 – 1599 (2000).
19. M. Xiao, Y. Ding, *Contact kinematics between three-dimensional rigid bodies with general surface parameterization*, J. Mech. Robot.; DOI: https://doi.org/10.1115/1.4048916.
20. L. Cui, D. Wang, J. S. Dai, *Kinematic geometry of circular surfaces with a fixed radius based on Euclidean in variants*, J. Mech. Des., **131**, 101001 – 101008 (2009).
21. L. Cui, J. S. Dai, *From sliding-rolling loci to instantaneus kinematics: an adjoint approach*, Mech. and Mach. Theory, **85**, 161 – 171(2015).
22. L. Cui, S. J. Dai, *A polynomial formulation of inverse kinematics of rolling contact*, J. Mech. Robot., **7**, № 4 (2015); https://doi.org/10.1115/1.4029498.
23. E. Cartan, *Riemannian geometry in an orthogonal frame*, World Scientific Press, Singapore (2002).
24. H. Cartan, *Differential forms*, Dover Publisher, New York (1996).
25. L. Cui, J. S. Dai, *Reciprocity-based singular value decomposition for inverse kinematic analysis of the metamorphic multi fingered hand*, J. Mech. Robot., **4**, 034502 – 034506 (2012).
26. A. Weiss, R. G. Langlois, M. J. D. Hayes, *Unified treatment of the kinematic interface between a sphere and omnidirectional wheel actuators*, J. Mech. Robot., **3**, 041001 – 041009 (2011).
27. M. Tosun, M. A. Gungor, I. Okur, *On the one-parameter Lorentzian spherical motions and Euler – Savary formula*, J. Appl. Mech., **74**, № 5, 972 (2007).
28. M. Aydınalp, M. Kazaz, H.H. Ugurlu, *The invers kinematics of rolling contact of timelike curves lying on timelike surfaces in Lorentzian 3-space*, Commun. Fac. Sci. Univ. Ank. Sér. A1 Math. Stat., **68**, 1879 – 1894 (2019).
29. J. S. Dai, D. Wang, L. Cui, *Orientation and workspace analysis of the multifingered metamorphic hand-metahand*, IEEE Trans. Robot., **25**, № 4, 942 – 947 (2009).
30. L. Cui, U. Cupcic, J. S. Dai, *An optimization approach to teleoperation of the thumb of a humanoid robot hand: kinematic mapping and calibration*, J. Mech. Des., **136**, 091005 – 091005 (2014).
31. J. Hu, M. Wang, T. Zan, *The kinematics of ball-screw mechanisms via the slide-roll ratio*, Mech. and Mach. Theory, **79**, 158 – 172 (2014).
32. G. Fekete, P. De Baets, M. Wahab, B. Csizmadia, G. Katona, L. V. Vanegas-Useche, J. A. Solanilla, *Sliding-rolling ratio during deep squat with regard to different knee prostheses*, Acta Polytech. Hungar., **9**, № 5, 5 – 24 (2012).
33. W. Pu, D. Zhu, J. Wang, Q. J. Wang, *Rolling-sliding contact fatigue of surfaces with sinusoidal roughness*, Int. J. Fatigue, **90**, 57 – 68 (2016).
34. J. Xie, J. Xu, W. Shang, K. Zhang, *Mode selection between sliding and rolling for droplet on inclined surface: effect of surface wettability*, Int. J. Heat and Mass Transfer, **122**, 45 – 58 (2018).
35. Y. Liu, M. Kong, N. Wan, P. Ben-Tzvi, *A geometric approach to obtain the closed-form forward kinematics of H4 parallel robot*, J. Mech. Robot., **10**, № 5 (2018).
36. A. T. Yang, G. R. Pennock, L. Hsia, *Instantaneous invariants and curvature analysis of a planar Four – Link mechanism*, J. Mech. Des., **116**, № 4, 1173 – 1176 (1994); https://doi.org/10.1115/1.2919504.
37. C. L. Chan, K. L. Ting, *Curvature theory on contact and transfer characteristics of enveloping curves*, in: Proceedings of the ASME 2018 International Design Engineering Technical Conferences and Computers and Information in Engineering Conference, vol. 5B, Quebec City, Quebec, Canada, August 26 – 29 (2018); https://doi.org/10.1115/DETC2018-86378.

Received 22.05.23